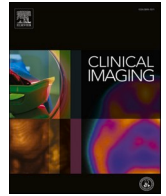




Since January 2020 Elsevier has created a COVID-19 resource centre with free information in English and Mandarin on the novel coronavirus COVID-19. The COVID-19 resource centre is hosted on Elsevier Connect, the company's public news and information website.

Elsevier hereby grants permission to make all its COVID-19-related research that is available on the COVID-19 resource centre - including this research content - immediately available in PubMed Central and other publicly funded repositories, such as the WHO COVID database with rights for unrestricted research re-use and analyses in any form or by any means with acknowledgement of the original source. These permissions are granted for free by Elsevier for as long as the COVID-19 resource centre remains active.



Cardiothoracic Imaging

Correlation of chest radiography findings with the severity and progression of COVID-19 pneumonia

Anas S. Al-Smadi^a, Akash Bhatnagar^a, Rehan Ali^{a,*}, Nicholas Lewis^b, Samuel Johnson^a^a Department of Radiology, Wayne State University, School of Medicine, Detroit, MI, USA^b Department of Radiology, John D. Dingell VA Medical Center, Detroit, MI, USA

ARTICLE INFO

Keywords:

COVID infection
Pneumonia
Viral pneumonia
Prognostication
Ground glass opacities and consolidation

ABSTRACT

Purpose: Aim is to assess the temporal changes and prognostic value of chest radiograph (CXR) in COVID-19 patients.

Material and methods: We performed a retrospective study of confirmed COVID-19 patients presented to the emergency between March 07–17, 2020. Clinical & radiological findings were reviewed. Clinical outcomes were classified into critical & non-critical based on severity. Two independent radiologists graded frontal view CXRs into COVID-19 pneumonia category 1 (CoV-P1) with <4 zones and CoV-P2 with ≥4 zones involvement. Inter-observer agreement of CoV-P category for the CXR preceding the clinical outcome was assessed using Kendall's τ coefficient. Association between CXR findings and clinical deterioration was calculated along with temporal changes of CXR findings with disease progression.

Results: Sixty-two patients were evaluated for clinical features. 56 of these (total: 325 CXRs) were evaluated for radiological findings. Common patterns were progression from lower to upper zones, peripheral to diffuse involvement, & from ground glass opacities to consolidation. Consolidations starting peripherally were noted in 76%, 93% and 48% with critical outcomes, respectively. The interobserver agreement of the CoV-P category of CXRs in the critical and non-critical outcome groups were good and excellent, respectively (τ coefficient = 0.6 & 1.0). Significant association was observed between CoV-P2 and clinical deterioration into a critical status ($\chi^2 = 27.7$, $p = 0.0001$) with high sensitivity (95%) and specificity (71%) within a median interval time of 2 days (range: 0–4 days).

Conclusion: Involvement of predominantly 4 or more zones on frontal chest radiograph can be used as predictive prognostic indicator of poorer outcome in COVID-19 patients.

1. Introduction

The pandemic pneumonia caused by 2019 novel Coronavirus (2019-nCoV) grew exponentially in the United States as it approaches its peak in multiple localities which has led to shortages of personal protective equipment, increased demand for ventilators, and prompted health care providers to make difficult decisions in the face of limited hospital beds and resources. Investigators are eager to understand the value of imaging for the screening, diagnosis and management of patients with known or suspected COVID-19 infection [1].

Previous publications have described the role of Chest computed tomogram (CT) in early diagnosis, predicting the severity and monitoring the progression of the disease [2–5], however, professional organizations such as the American College of Radiology (ACR) have

classified its role as “usually not appropriate” for acute respiratory illness hence recommends the CT should be used sparingly [6].

Chest radiograph (CXR) played a role in determining the course and the severity of disease during the 2002 severe acute respiratory syndrome (SARS) and the 2012 Middle East respiratory syndrome (MERS) outbreaks [7]. Since prior reports have studied the role of clinical factors in predicting COVID-19 disease severity and mortality such as age, comorbidities and various laboratory and inflammatory parameters [8,9], we will focus in this study on evaluating the correlation of CXR findings with COVID-19 disease course and severity outcome which may assist the clinicians in predicting the clinical course of patient's disease based on CXR imaging findings.

* Corresponding author at: Department of Radiology, Wayne State University, School of Medicine, 4201 St. Antoine, DRH, 3L-8, Detroit, MI 48201, USA.
E-mail address: rehanali253@gmail.com (R. Ali).

2. Materials and methods

2.1. Patient study and image acquisition

2.1.1. Study population

Institutional review board approval was obtained for a retrospective study of patients with Reverse transcription polymerase chain reaction (RT-PCR) confirmed 2019-nCoV infection who presented to the emergency department from March 07, 2020 to March 17, 2020. A waiver of informed patient consent was granted by the ethics committee. Patients without CXR were excluded from imaging and statistical analysis.

2.1.2. Clinical data analysis

We collected clinical data including demographics, past medical history, presenting complaint and other symptoms, history of contact exposure, and hospital course.

The clinical severity outcomes of COVID-19 patients were classified, based on the seventh edition of the China Guidelines for the Diagnosis and Treatment Plan of Novel Coronavirus (2019-nCoV) Infection by the National Health Commission and U.S. Center for Disease Control and Prevention (CDC) Clinical Guidance for Management of Patients with Confirmed Coronavirus Disease as detailed into *critical status*, if the patient developed severe or critically severe symptoms during hospital course, and *non-critical status*, if the patient was discharged after improvement or resolution of symptoms (Table 1) [10,11].

2.2. Imaging study analysis

Images were independently reviewed on a de-identified Picture archiving and communication system (PACS) by two experienced radiologists (SJ and NL with 23 and 5 years of experience) respectively. To minimize bias, the reviewers were blinded to the clinical data other than COVID-19 positivity. All patients had a CXR using digital portable anteroposterior (AP) technique per hospital protocol to minimize in-hospital transmission through the radiology department. Inter-observer disagreements on CXR findings were resolved by consensus or third radiologist.

Radiographic features were described according to Fleischner Society glossary of terms including ground glass opacity (GGO) and consolidation [12–14]. Each lung was divided into three zones. The upper zone extends from the apex to the lower border of the anterior second rib or to the superior hilar markings, middle zone from the lower border of anterior 2nd rib to lower border of anterior 4th rib or from the superior hilar markings to the inferior hilar markings, and the lower zone from the lower border of anterior 4th rib to the lung base or from the inferior hilar markings to lung base (Fig. 1A). Each zone involvement was assigned 1 point with a total score of 6. The CXRs were then classified to one of two categories: COVID-19 pneumonia 1 (CoV-P1) if total score < 4 and COVID-19 pneumonia 2 (CoV-P2) if total score \geq 4. We followed the temporal changes of CXR findings as well.

Table 1
Clinical outcome according to severity

Category	Severity	Criteria
Non-critical	Mild	No dyspnea, no asthma, with or without cough, no underlying chronic diseases, e.g.: heart, lung and kidney diseases, low grade fever
	Moderate	Mild symptoms with dyspnea, high grade fever, underlying respiratory or other chronic diseases
	Severe	Respiratory distress with RR > 30 times/min, oxygen saturation at rest <93%, or PaO ₂ /FiO ₂ < 300 mmHg
Critical	Critically severe	Respiratory failure needing mechanical ventilation, shock, or combination with other organ failure needing ICU intensive care

2.3. Statistical analysis

The receiver operating characteristic (ROC) curve for the clinical outcome with respect to CXR summed scores was used to determine the dividing point achieving high sensitivity and specificity to be used as cut-off value for CoV-P category classification. Baseline CXRs at presentation and the first CXR, based on consensus, that met the definition of a CoV-P2 category along the course of each patient's disease were included in the statistical analysis. Interobserver agreement in the lung zone involvement score and the CoV-P category were assessed using Kendall's τ coefficient.

Levels of agreement range from 0 to 1, where a level of 0.8 or greater represented excellent agreement; a level of 0.5 or greater to less than 0.8, good agreement; a level of 0.2 or greater to less than 0.5, fair agreement; and a level of less than 0.2, poor agreement. A *p*-value of <0.05 indicated a statistically significant agreement.

The statistical difference of the CoV-P category of chest radiograph preceding the clinical outcome, whether critical or non-critical, was tested using Chi-square test. The mean, median and mode of the time difference between the first CXR that met the definition of a CoV-P2 category and clinical deterioration to a critical status outcome were reported. A *p*-value of <0.05 indicated a statistically significant difference. Statistical analysis was performed using SPSS statistical software (V.26.0, 2019 SPSS Inc).

3. Results

3.1. Patient demographics and presentations

A total of 62 patients (male vs female: 33 and 29) with confirmed 2019-nCoV presented to the emergency department during the study period with a mean age of 57.9 years (range: 25–95). Cough, fever and shortness of breath were the most prevalent presenting symptoms (71%, 62% and 44% respectively). Eighteen patients (29%) presented with GI symptoms of abdominal pain, diarrhea and vomiting, and 13 patients presented with neurological symptoms (21%), including one with focal seizure. One patient reported loss of taste sensation. Cardiovascular disease was the most prevalent co-morbidity (65%) followed by diabetes (45%), and chronic obstructive lung disease including asthma (26%). Interestingly, only 13 of the 62 patients (21%) reported a history of ill contact (Table 2).

Sixteen of 62 patients (26%) passed away with mean age of 63.3 \pm 11.7 years (range: 47–95, M:F = 9:7) Of these, 10 had type 2 diabetes (63%), 10 had cardiovascular disease (63%), 6 had chronic respiratory disease (38%), and 4 had chronic kidney disease (25%). Among these patients, 75% had at least 2 of these co-morbidities.

3.2. Imaging study findings

Six patients did not have CXRs, hence, only 56 patients were included in the imaging and statistical analysis. A total of 325 CXRs were reviewed.

There were 56 baseline CXRs at presentation (Fig. 1) with radiologic features detailed (Table 3). The most common pattern of baseline CXRs, irrespective of the CoV-P category, was GGO (56%) followed by mixed pattern (23%) and consolidation (7%). Eight patients (14%) had normal baseline CXRs. The majority of patients had bilateral findings (86%) and lower predominant (middle and lower zones) (89%) on baseline CXRs. Six baseline CXRs had a peripheral distribution (11%), while 89% had no transverse predilection to either peripheral or perihilar distribution.

Among the 56 baseline CXRs, 27 CXRs were categorized as CoV-P1 (Table 4). Eight of these CXRs were normal (30%). The most common pattern was GGO (56%). One CXR had consolidation pattern involving 2 zones (4%), and this patient developed critical outcome before meeting the criteria of CoV-P2 category (false positive). All CXRs had predominantly lower zones involvement and the majority did not show

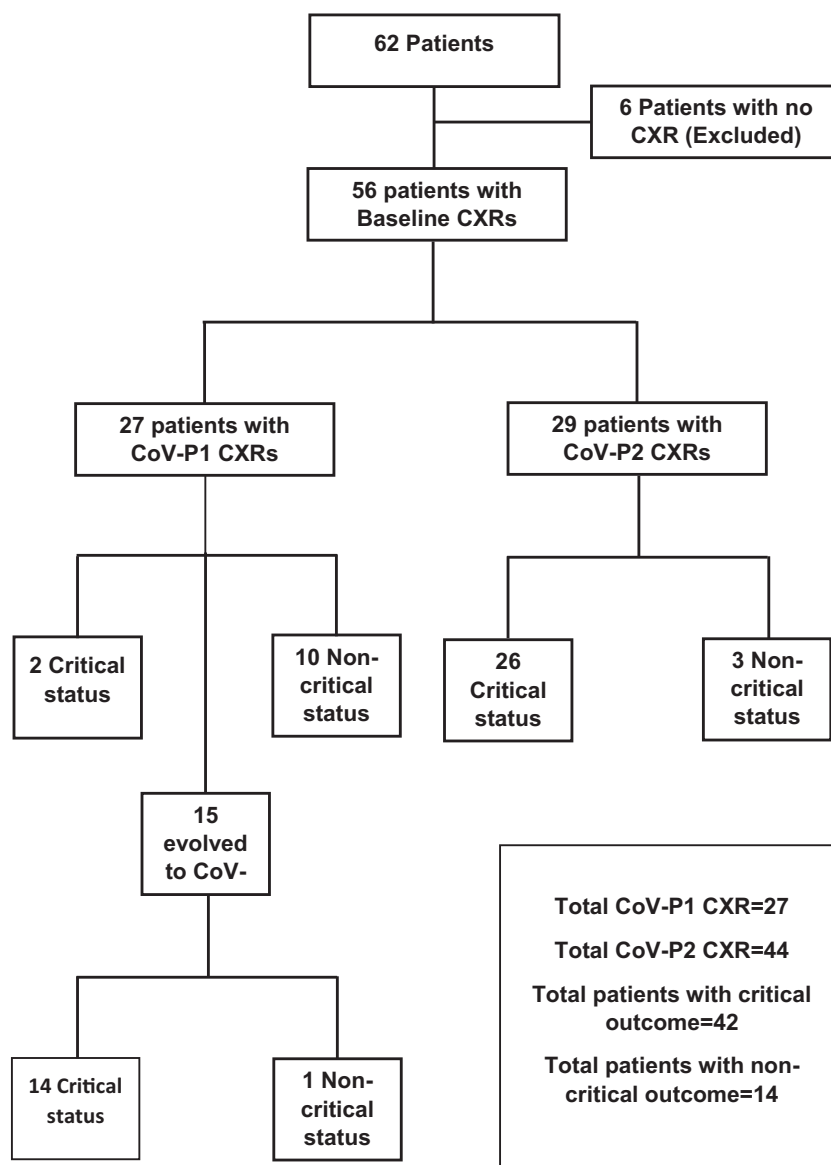


Fig. 1. Diagram of retrospective review of baseline and follow-up CXRs.

predilection of transverse distribution (85%). Two of these 27 CXRs (7%) eventually developed diffuse involvement of 5 and 6 zones, both were the false positives that deteriorated to a critical status without CoV-P2 CXR (false positives), as demonstrated (Fig. 1). One of these false positives had consolidation only, as mentioned earlier, and the other had mixed pattern involving 3 zones with area of peripheral consolidation in the right lower and middle zones of the chest radiograph.

For each of the 56 patients, we identified the first CXR that met the definition of a CoV-P2 category among baseline and follow-up CXRs, which yielded 44 CXRs (Table 5). Mixed pattern of both consolidation and GGO was the most common pattern (52%). 39 of these CXRs (89%) evolved to a predominantly consolidative pattern on follow up CXRs. In 20/44 CoV-P2 CXRs (45%), the consolidation started peripherally then became diffuse (Figs. 1C and 2C). Five of the 44 CoV-P2 CXRs maintained a mixed pattern without evolving to a consolidative pattern; four of these were not associated with a critical outcome (false positives). Among these 44 CXRs, 30 (68%) eventually developed diffuse involvement of all 6 zones on subsequent images.

Among the 10 patients with combined CoV-P1 CXR and non-critical outcomes (Fig. 1), 4 were discharged home from ED and 6 were admitted and maintained CoV-P1 on follow-up CXRs. Only 2 patients

with CoV-P1 CXRs deteriorated to a critical outcome without developing CoV-P2 CXR (false negatives). Of the 42 patients with critical outcome, 40 (95%) had a CoV-P2 CXR preceding the clinical deterioration by a mean time of 1.8 days (an example of this is illustrated in Fig. 3). Thirty two of 42 patients with critical outcome eventually developed diffuse involvement of all zones (76%), 39 eventually developed predominantly consolidative patterns (93%), and 20 patients of these had areas of consolidation starting peripherally (48%). Twenty two of 56 patients (39%) evolved into clinical and radiologic acute respiratory distress syndrome (ARDS). None of the patients had cavitation or demonstrable pleural effusion on CXR.

3.3. Statistical and interobserver analysis

The ROC curve for the outcome with respect to CXR score showed a dividing point with high sensitivity and specificity is 4 zones of involvement (Sensitivity of 0.9 and specificity of 0.71), so it was used as a cut-off value for CoV-P category classification. With respect to critical status, inter-observer agreement in the CXR score and the resulting CoV-P category were fair (τ coefficient = 0.3, $P = 0.001$) and good (τ coefficient = 0.6, $P = 0.000$), respectively. With respect to non-critical

Table 2
Patient demographics and clinical features

Criteria	Number of patients (%)
Age	57.9 ± 16.1
Male	33 (53%)
Female	29 (47%)
History of contact	13 (21%)
Symptoms/signs at presentation	
Fever	38 (62%)
Cough	44 (71%)
Chest pain	11 (18%)
SOB	27 (44%)
Chills	16 (26%)
Arthralgia/myalgia/fatigue	14 (23%)
GI symptoms	18 (29%)
Headache	12 (19%)
seizure	1 (2%)
Co-morbidities	
COPD	10 (16%)
Asthma	6 (10%)
Cardiovascular disease	40 (65%)
DM	28 (45%)
Immunocompromised	6 (10%)
Pregnancy	1 (2%)
Renal disease	6 (10%)
Death	16 (26%)

(COPD: Chronic obstructive pulmonary disease, SOB: Shortness of breath, GI: Gastrointestinal, DM: Diabetes mellitus).

Table 3
Baseline chest X-ray CXR features (56 CXRs)

Baseline CXR feature	Number of cases	%
Pattern		
Normal	8	14%
GGO	31	56%
Consolidation	4	7%
Mixed	13	23%
CoV-P category		
CoV-P1	27	48%
CoV-P2	29	52%
Lung involvement among CXRs with positive findings (48)		
Unilateral	8	14%
Bilateral	48	86%
Vertical distribution among CXRs with positive findings (48)		
Lower predominant	50	89%
Upper predominant	0	0%
Diffuse involvement	6	11%
Transverse distribution among CXRs with positive findings (48)		
Peripheral	6	11%
Perihilar	0	0%
No predilection	50	89%

(GGO = Ground Glass Opacities).

status, inter-observer agreement in the CXR score and the resulting CoV-P category were fair (τ coefficient = 0.4, $P = 0.005$) and excellent (τ coefficient = 1.0, $P = 0.000$), respectively.

There was disagreement on CoV-P category in 3 cases, which was resolved by consensus. There was a statistically significant difference in CoV-P category between the critical and non-critical status ($\chi^2 = 27.7$, $P = 0.000$) (Table 6). This indicates that the CoV-P2 category is more likely to be associated with deterioration into a critical clinical status with 95% sensitivity, 71% specificity and 89% accuracy. The mean, median and mode interval between the first encountered CXR with CoV-P2 findings and clinical deterioration to a critical status were 1.8, 2 and 1 days, respectively (range 0–4 days; mean standard deviation and variance are 1.2 and 1.5 respectively). Patients with 0 days interval either presented to emergency with CoV-P2 or did not have regular follow-up CXRs.

Table 4
COVID Pneumonia CoV-P1 CXR features (27 CXRs)

CoV-P1 CXR features	Number of cases	%
Pattern		
Normal	8	30%
GGO	15	56%
Consolidation	1	4%
Mixed	3	10%
Lung involvement		
Unilateral	8	30%
Bilateral	19	70%
Vertical distribution		
Lower predominant	27	100%
Upper predominant	0	0%
Diffuse involvement	0	0%
Transverse distribution		
Peripheral	4	15%
Perihilar	0	0%
No predilection	23	85%

(GGO = Ground Glass Opacities)

Table 5
First encountered COVID Pneumonia (CoV-P2) chest X-ray (CXR) features (44 CXRs)

CoV-P2 CXR features	Number of cases	%
Pattern		
GGO	15	34%
Consolidation	6	14%
Mixed	23	52%
Lung involvement		
Unilateral	0	0%
Bilateral	44	100%
Vertical distribution		
Lower predominant	33	75%
Upper predominant	0	0%
Diffuse involvement	11	25%
Transverse distribution		
Peripheral	0	0%
Perihilar	0	0%
No predilection	44	100%
Peripheral consolidation	20	45%

(GGO = Ground Glass Opacities)

4. Discussion

Early literature from China focused on the CT findings as a sensitive tool to diagnose and follow up COVID-19 patients [5,15,16]. As we developed a better understanding of the nature of this disease, various clinical features and laboratory tests (e.g. normal WBC count, lymphopenia, elevated LDH, prolonged prothrombin time, elevated CPK and elevated D-Dimer) collectively direct clinicians to suspect COVID-19 while awaiting RT-PCR results, despite often normal initial CXR imaging [16,17]. Chest CTs are now reserved for certain scenarios in which CT might alter the treatment plan, as described in a recent multinational consensus statement from the Fleischner Society [18]. In this study we comprehensively evaluated the value of CXR findings as an adjunct to help clinicians make decisions in suspected cases in the emergency room setting, as well as in admitted patients with confirmed COVID-19.

Our study demonstrated common patterns in the evolution of CXR findings with disease severity progression from GGO to predominantly consolidative and from lower zones involvement to diffuse. A common pattern of consolidation was noted to start peripherally. The vertical distribution and peripheral areas of consolidation noted in our study are in keeping with previous reports [13,19,20]. This expected temporal evolution of COVID-19 is comparable to previous studies of SARS and MERS that demonstrated ill-defined areas of airspace opacity in lower

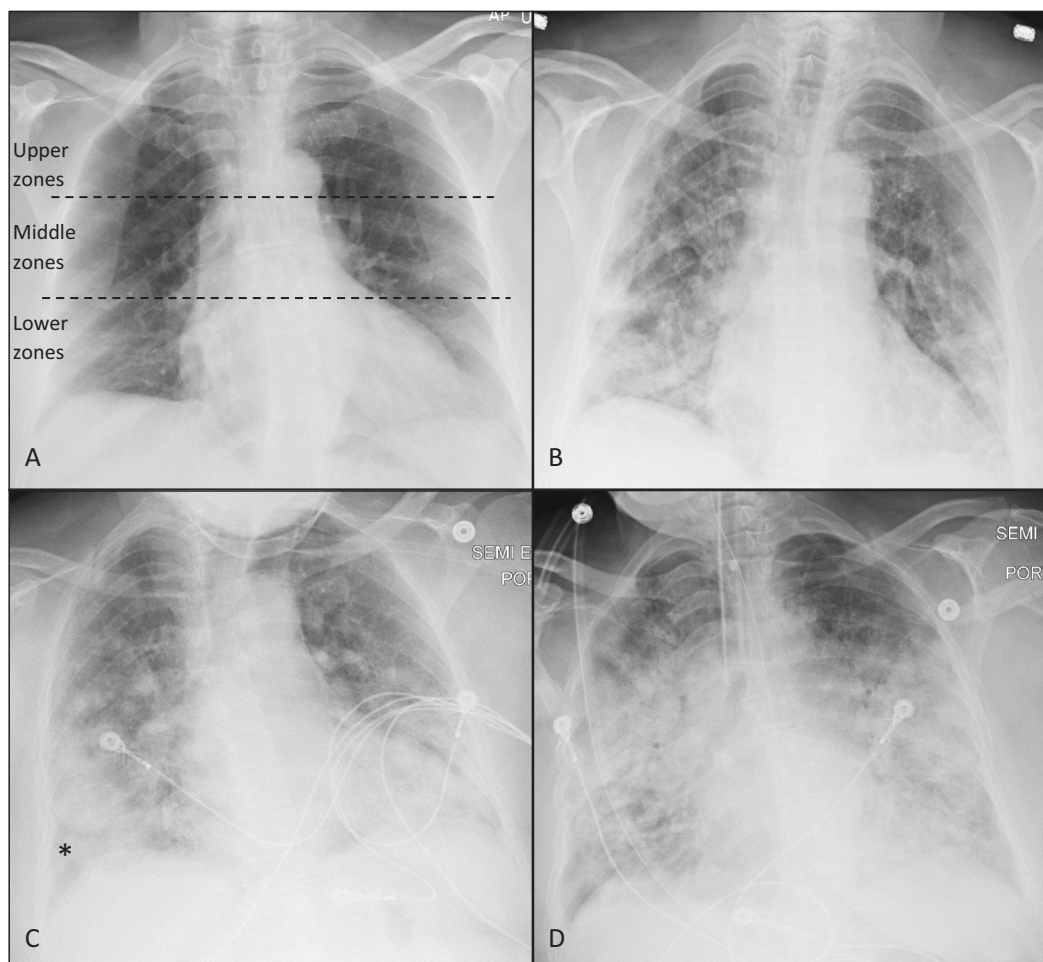


Fig. 2. AP chest radiographs of a 65 years-old female presented with moderate symptoms. Hypertension was the only co-morbidity. Both observers assigned CoV-P1 category to the baseline CXR with GGO involving bilateral lower zones (A). GGO became more extensive 2 days later (B) with CoV-P2 category assigned by both observers (4 and 5 zones were considered involved by each observer) with increased consolidation component. There was no significant change in clinical status other than improvement of shortness of breath reported by the patient at the time of this CXR. Patient deteriorated clinically on the third day with severe symptoms and was transferred to the intensive care unit. CXR on the fourth day (C) shows more extensive involvement with increased consolidation noted mainly peripherally (*). Patient was intubated 6 days after admission (critically severe) and developed ARDS features (D).

lung zones initially, which progress in follow-up images into consolidation involving both lungs and extend to involve the upper lobes, in addition to lack of pleural effusion or cavitation [21–23].

In our study, we evaluated the correlation between the temporal changes of CXR findings and the severity and the course of the disease. CoV-P2 was significantly associated with clinical deterioration to a critical status ($\chi^2 = 27.7, P = 0.000$) within a median interval time of 2 days (range 0–4 days). The sensitivity and specificity were 95% and 71%, respectively. Similar to our study, *Antonio* et al. showed that the number of opacified lung zones in SARS patients was a predictive prognostic indicator of mortality with two thirds of those patients who died had involvement of 4 or more zones [24]. *Toussie* et al. described the predictive value of initial CXR on admission and concluded that involvement of ≥ 3 zones in COVID-19 patients is associated with worse outcomes, however this study targeted younger adults aged 21–50 years old [20]. We had 2 false positives only, one of them had areas of consolidation involving 2 zones only and the other had mixed pattern with peripheral area of consolidation involving 2 zones. This may indicate the importance of consolidation early in the disease besides the extent of CXR involvement in predicting poor outcome.

Patients with 0-day interval between CoV-P2 CXR and critical outcome were either presented to ED with severe/critically severe symptoms or did not have regular follow-up CXRs during

hospitalization. Therefore, daily or every other day CXR may provide predictive value of clinical status in inpatient setting. However, based on our dataset, we consider daily CXRs in the ICU setting of limiting utility, given that it will not change clinical management, rather will instead increase risk of exposure to radiology personnel.

Recent literature shows promising utilization of artificial intelligence (AI)-driven tools in the screening and diagnosis of COVID-19 pneumonia. An example of the former application is Truncated Inception Net that is being proposed as a screening tool for COVID-19 outbreak using chest x-rays taking advantage of the AI-driven tools active-learning based on cross-population train/test models that utilize multitudinal and multimodal data [25,26]. An example of the diagnostic application is CV19-Net that was able to diagnose COVID-19 pneumonia and differentiate it from non-COVID-19 pneumonia using CXR with high sensitivity and specificity [27]. An area of future research is to utilize this data set to design an AI based algorithm to predict clinical deterioration using radiographic images.

Potential strengths of our studies include imaging and clinical findings integration, homogenous nature of cohort, availability of data points and less attrition biases. Our results are subject to the inherent limitations of a retrospective study, single center based, small time period, and semi-quantitative grading of CXR images. We attempted to mitigate this bias with blinded observer analysis, and a protocol for

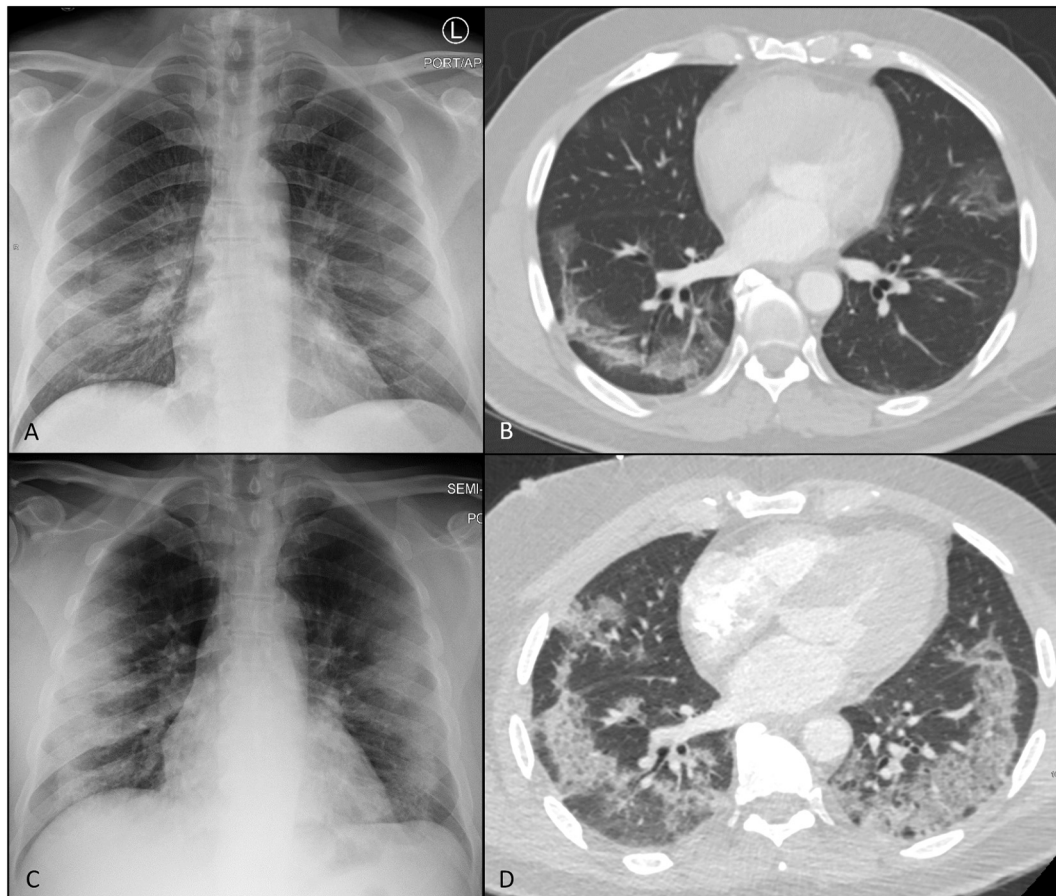


Fig. 3. Baseline CXR (A) demonstrates GGO involving mainly the lower zones and was assigned CoV-P1 by both observers. Lower lungs seen on CT abdomen/pelvis (B), that was ordered for diarrhea and abdominal pain, demonstrates bilateral GGO. CXR on emergency re-visit for mild respiratory symptoms (C) demonstrates interval development of bilateral areas of consolidation, mainly peripherally, involving predominantly 4 zones and was assigned CoV-P2 by both observers. CTPA for clinical suspicion of pulmonary embolism (D) demonstrates interval development of crazy-paving with increased extension of the disease, however was negative for pulmonary embolism. The patient deteriorated into a critical status 3 days following CoV-P2 CXR.

Table 6
Correlation between COVID Pneumonia (CoV-P) category and clinical outcome

CXR category	Critical	Non-critical	Total
CoV-P1	2	10	12
CoV-P2*	40	4	44
Total	42	14	56
	* $\chi^2 = 27.7$	P = 0.000	
	Sensitivity	95%	
	Specificity	71%	
	Accuracy	89%	

grading CXR findings. Furthermore, memory bias was limited with the large number of CXRs and only 2 observers from a large group of 30 radiologists involved in the initial diagnostic reporting of these images. Selection bias is another limitation with inclusion of only patients presented to the emergency and hospitalized patients granted lack of clinical or radiological follow up for outpatients. In addition, lack of daily CXRs on some patients in this study may affect the observed versus true interval between CoV-P2 and clinical deterioration. Future studies with a larger population of inpatients and outpatients would require a multi-institutional cohort, as well as regular clinical and radiological follow up.

5. Conclusion

We evaluated the temporal evolution and correlation of chest

radiograph findings to deterioration into a severe or critically severe clinical status. Involvement of predominantly 4 or more zones on frontal chest radiograph can predict clinical deterioration within a median interval time of 2 days with high accuracy (89%). Thus, chest radiograph can be used as an adjunctive prognostic indicator, in addition to other clinical information and laboratory tests, in guiding further treatment and resource allocation.

CRedit authorship contribution statement

Study concept and design: AA, AB, NL, SJ.
 Acquisition of data: AA, AB, NL, SJ.
 Analysis and interpretation of data: All Authors.
 Drafting of the manuscript: AA, AB, RA.
 Critical revision of the manuscript for important intellectual content: All Authors.
 Statistical analysis: AA, AB, RA.
 Administrative, technical, or material support: AA, AB, SJ.
 Study supervision: AA, NL, SJ.

Declaration of competing interest

None of the authors report any disclosure. This research did not receive any specific grant from funding agencies in the public, commercial, or not-for-profit sectors.

References

- [1] Ranney ML, Griffith V, Jha AK. Critical supply shortages — the need for ventilators and personal protective equipment during the Covid-19 pandemic 2020;382(18): e41. <https://doi.org/10.1056/NEJMp2006141>.
- [2] Salehi S, Abedi A, Balakrishnan S, Gholamrezaezhad A. Coronavirus disease 2019 (COVID-19): a systematic review of imaging findings in 919 patients. *Am J Roentgenol* 2020;1–7. <https://doi.org/10.2214/AJR.20.23034>.
- [3] Ai T, Yang Z, Hou H, Zhan C, Chen C, Lv W, Tao Q, Sun Z, Xia L. Correlation of chest CT and RT-PCR testing in coronavirus disease 2019 (COVID-19) in China: a report of 1014 cases. *Radiology*;0(0):200642. doi:<https://doi.org/10.1148/radiol.2020200642>.
- [4] Xie XZ, Zhong Z, Zhao W, et al. Chest CT for typical 2019-nCoV pneumonia: relationship to negative RT-PCR testing. *Radiology* 2020;296(2):E41–5. <https://doi.org/10.1148/radiol.2020200343>.
- [5] Zhao W, Zhong Z, Xie X, Yu Q, Liu J. Relation between chest CT findings and clinical conditions of coronavirus disease (COVID-19) pneumonia: a multicenter study. *Am J Roentgenol* 2020;1–6. <https://doi.org/10.2214/AJR.20.22976>.
- [6] ACR. Recommendations for the use of chest radiography and computed tomography (CT) for suspected COVID-19 infection. ACR: American College of Radiology; 2020.
- [7] Hosseiny M, Kooraki S, Gholamrezaezhad A, Reddy S, Myers L. Radiology perspective of coronavirus disease 2019 (COVID-19): lessons from severe acute respiratory syndrome and Middle East respiratory syndrome. *AJR Am J Roentgenol* 2020;214(5):1078–82. <https://doi.org/10.2214/ajr.20.22969>.
- [8] Du R-H, Liang L-R, Yang C-Q, Wang W, Cao T-Z, Li M, et al. Predictors of mortality for patients with COVID-19 pneumonia caused by SARS-CoV-2: a prospective cohort study. *Eur Respir J* 2020;2000524. <https://doi.org/10.1183/13993003.00524-2020>.
- [9] Ruan Q, Yang K, Wang W, Jiang L, Song J. Correction to: clinical predictors of mortality due to COVID-19 based on an analysis of data of 150 patients from Wuhan, China. *Intensive Care Med* 2020. <https://doi.org/10.1007/s00134-020-06028-z>.
- [10] Wu Z, McGoogan JM. Characteristics of and important lessons from the coronavirus disease 2019 (COVID-19) outbreak in China: summary of a report of 72314 cases from the Chinese Center for Disease Control and Prevention. *Jama* 2020. <https://doi.org/10.1001/jama.2020.2648>.
- [11] Xu Y-H, Dong J-H, An W-M, Lv X-Y, Yin X-P, Zhang J-Z, et al. Clinical and computed tomographic imaging features of novel coronavirus pneumonia caused by SARS-CoV-2. *J Infect* 2020;80(4):394–400. <https://doi.org/10.1016/j.jinf.2020.02.017>.
- [12] Hansell DM, Bankier AA, MacMahon H, McLoud TC, Muller NL, Remy J. Fleischner society: glossary of terms for thoracic imaging. *Radiology* 2008;246(3):697–722. <https://doi.org/10.1148/radiol.2462070712>.
- [13] Wong HYF, Lam HYS, Fong AH-T, Leung ST, Chin TW-Y, Lo CSY, Lui MM-S, Lee JCY, Chiu KW-H, Chung T, Lee EYP, Wan EYF, Hung FNI, Lam TPW, Kuo M, Ng M-Y. Frequency and distribution of chest radiographic findings in COVID-19 positive patients. *Radiology*;0(0):201160. doi:<https://doi.org/10.1148/radiol.2020201160>.
- [14] Rodrigues JCL, Hare SS, Edey A, Devaraj A, Jacob J, Johnstone A, et al. An update on COVID-19 for the radiologist - a British society of thoracic imaging statement. *Clin Radiol* 2020;75(5):323–5. <https://doi.org/10.1016/j.crad.2020.03.003>.
- [15] Pan F, Ye T, Sun P, Gui S, Liang B, Li L, Zheng D, Wang J, Hesketh RL, Yang L, Zheng C. Time course of lung changes on chest CT during recovery from 2019 novel coronavirus (COVID-19) pneumonia. *Radiology*;0(0):200370. doi:<https://doi.org/10.1148/radiol.2020200370>.
- [16] Goh KJ, Choong MC, Cheong EH, Kalimuddin S, Duu Wen S, Phua GC, et al. Rapid progression to acute respiratory distress syndrome: review of current understanding of critical illness from COVID-19 infection. *Ann Acad Med Singapore* 2020;49(1):1–9.
- [17] Singhal T. A review of coronavirus disease-2019 (COVID-19). *The Indian Journal of Pediatrics* 2020;87(4):281–6. <https://doi.org/10.1007/s12098-020-03263-6>.
- [18] Rubin GD, Ryerson CJ, Haramati LB, Sverzellati N, Kanne JP, Raouf S, Schluger NW, Volpi A, Yim J-J, Martin IBK, Anderson DJ, Kong C, Altes T, Bush A, Desai SR, Goldin J, Goo JM, Humbert M, Inoue Y, Kauczor H-U, Luo F, Mazzone PJ, Prokop M, Remy-Jardin M, Richeldi L, Schaefer-Prokop CM, Tomiyama N, Wells AU, Leung AN. The role of chest imaging in patient management during the COVID-19 pandemic: a multinational consensus statement from the Fleischner society. *Radiology*;0(0):201365. doi:<https://doi.org/10.1148/radiol.2020201365>.
- [19] Soon Ho Yoon M, Lee Kyung Hee, Kim Jin Yong, Lee Young Kyung, Ko Hongseok, Kim Ki Hwan, et al. Chest radiographic and CT findings of the 2019 novel coronavirus disease (COVID-19): analysis of nine patients treated in Korea. *Korean J Radiol* 2020;21(4):494–500.
- [20] Toussie D, Voutsinas N, Finkelstein M, Ceditillo MA, Manna S, Maron SZ, et al. Clinical and chest radiography features determine patient outcomes in young and middle age adults with COVID-19. *Radiology* 2020;201754. <https://doi.org/10.1148/radiol.2020201754>.
- [21] Wong KT, Antonio GE, Hui DS, Lee N, Yuen EH, Wu A, et al. Severe acute respiratory syndrome: radiographic appearances and pattern of progression in 138 patients. *Radiology* 2003;228(2):401–6. <https://doi.org/10.1148/radiol.2282030593>.
- [22] Paul NS, Roberts H, Butany J, Chung T, Gold W, Mehta S, et al. Radiologic pattern of disease in patients with severe acute respiratory syndrome: the Toronto experience. *Radiographics: a review publication of the Radiological Society of North America, Inc* 2004;24(2):553–63. <https://doi.org/10.1148/rg.242035193>.
- [23] Das KM, Lee EY, Al Jawder SE. Acute Middle East respiratory syndrome coronavirus: temporal lung changes observed on the chest radio-graphs of 55 patients. *AJR* 2015;205(web):W267.
- [24] Antonio GE, Wong KT, Tsui EL, Chan DP, Hui DS, Ng AW, et al. Chest radiograph scores as potential prognostic indicators in severe acute respiratory syndrome (SARS). *AJR Am J Roentgenol* 2005;184(3):734–41. <https://doi.org/10.2214/ajr.184.3.01840734>.
- [25] Santosh KC. AI-driven tools for coronavirus outbreak: need of active learning and cross-population train/test models on multitudinal/multimodal data. *J Med Syst* 2020;44(5):93. <https://doi.org/10.1007/s10916-020-01562-1>.
- [26] Das D, Santosh KC, Pal U. Truncated inception net: COVID-19 outbreak screening using chest X-rays. *Australas Phys Eng Sci Med* 2020;43(3):915–25. <https://doi.org/10.1007/s13246-020-00888-x>.
- [27] Zhang R, Tie X, Qi Z, Bevins NB, Zhang C, Griner D, Song TK, Nadig JD, Schiebeler ML, Garrett JW, Li K, Reeder SB, Chen G-H. Diagnosis of COVID-19 pneumonia using chest radiography: value of artificial intelligence.0(0):202944. doi:<https://doi.org/10.1148/radiol.2020202944>.